Proposal for an Experiment at PSI

Precise Measurement of the $\pi^+ \to e^+\nu$ Branching Ratio

V. A. Baranov,[c] W. Bertl,[b] M. Bychkov,[a] Yu. M. Bystritsky,[c] E. Frlež,[a] V. A. Kalinnikov,[c]
N. V. Khomutov,[c] A. S. Korenchenko,[c] S. M. Korenchenko,[c] M. Korolija,[f] T. Kozlowski,[d]
N. P. Kravchuk,[c] N. A. Kuchinsky,[c] D. Mzhavia,[c,e] A. Palladino,[a] D. Počanić,[a,*]
P. Robmann,[g] O. A. Rondon-Aramayo,[a] A. M. Rozhdestvensky,[c] T. Sakhelashvili,[g,†]
S. Scheu,[g] V. V. Sidorkin,[c] U. Straumann,[g] I. Supek,[f] Z. Tsamalaidze,[e]
A. van der Schaaf,[g,*] E. P. Velicheva,[c] and V. P. Volnykh,[c]

[a] *Department of Physics, University of Virginia, Charlottesville, VA 22904-4714, USA*
[b] *Paul Scherrer Institut, CH-5232 Villigen PSI, Switzerland*
[c] *Joint Institute for Nuclear Research, RU-141980 Dubna, Russia*
[d] *Institute for Nuclear Studies, PL-05-400 Swierk, Poland*
[e] *Institute for High Energy Physics, Tbilisi, State University, GUS-380086 Tbilisi, Georgia*
[f] *Rudjer Bošković Institute, HR-10000 Zagreb, Croatia*
[g] *Physik Institut der Universität Zürich, CH-8057 Zürich, Switzerland*

[The *PEN* Collaboration]

6 January 2006

Summary: We are proposing a new measurement of the $\pi^+ \to e^+\nu(\gamma)$ (π_{e2} decay) branching ratio with a relative uncertainty of $\sim 5 \times 10^{-4}$ or lower, at PSI, using the PIBETA detector system. Well controlled theoretical uncertainties for the π_{e2} decay render this process the most accurate experimental test of lepton universality available. At present, accuracy of the π_{e2} decay measurements lags behind the theoretical precision by an order of magnitude. A number of exotic physics scenarios outside the standard model may lead to a violation of lepton universality. Lepton universality, and lepton properties in general, have acquired added significance in the light of developments in the neutrino sector. A stringent experimental test of electron–muon universality will remain relevant regardless of the path that future theoretical and experimental developments may take.

---

*Co-spokesmen.

†On leave from Institute for High Energy Physics, Tbilisi, Georgia.

BEAM REQUIREMENTS:

<u>Beam line</u>: πE1

<u>Beam properties</u>:

    particle type: π^+

    intensity: $\sim 1\,000 - 20\,000\ \pi^+/$s stopped in target

    momentum: $65 - 80\,\mathrm{MeV/c}$

<u>Detector</u>: the PIBETA detector system

<u>Special conditions</u>: Setup of the PIBETA DAQ shack inside the area, as during the 1999–2001 and 2004 runs, including the special shielding wall.

<u>Original beam request</u>: Six weeks, in the fall of 2006.

<u>Subsequent beam requests</u>: Several months of beam time in the πE1 area in 2007 and, likely, a run in 2008.

SPECIAL SAFETY CONSIDERATIONS: none

Note: The running conditions will be the same as during the 2004 PIBETA run, with a lower pion beam intensity.

1.   Physics motivation

Historically, the ratio of decay rates $\Gamma(\pi \to e\bar{\nu}(\gamma))/\Gamma(\pi \to \mu\bar{\nu}(\gamma))$ provided one of the key confirmations of the $V - A$ nature of the electroweak interaction.[‡] It is therefore not surprising that practically all modern textbooks on subatomic physics continue to treat the $\pi \to \ell\bar{\nu}_\ell$ decay in detail at the tree level. Furthermore, higher-order contributions to the process are so well controlled that the ratio can be calculated with the highest accuracy of any allowed meson decay. The two most recent standard model (SM) calculations are by Marciano and Sirlin [1] and Decker and Finkemeier [2]. They give, respectively,

$$R_{e/\mu}^{\mathrm{SM}} = \left.\frac{\Gamma(\pi \to e\bar{\nu}(\gamma))}{\Gamma(\pi \to \mu\bar{\nu}(\gamma))}\right|_{\mathrm{calc}} = \begin{cases} (1.2352 \pm 0.0005) \times 10^{-4}, & \text{Ref. [1], and} \\ (1.2356 \pm 0.0001) \times 10^{-4}, & \text{Ref. [2].} \end{cases}$$

These authors have demonstrated that the π_{e2} branching ratio is theoretically understood at the level of a few parts in 10^4, i.e., $(\Delta R/R)_{e/\mu}^{\mathrm{SM}} \leq 4 \times 10^{-4}$. Subsequently, Kuraev has discussed radiative contributions to $\pi \to e\nu$ decay at the 0.1 % level [3].

On the other hand, experimental results lag in precision behind the SM calculations by about an order of magnitude. The current world average, unchanged for a decade, gives the ratio [4]

$$R_{e/\mu}^{\mathrm{exp}} = \left.\frac{\Gamma(\pi \to e\bar{\nu}(\gamma))}{\Gamma(\pi \to \mu\bar{\nu}(\gamma))}\right|_{\mathrm{exp}} \equiv B(\pi \to e\bar{\nu}(\gamma))_{\mathrm{exp}} = (1.230 \pm 0.004) \times 10^{-4},$$

i.e., $(\Delta R/R)^{\mathrm{exp}} \simeq 33 \times 10^{-4}$, or about an order of magnitude less accurate than the standard model calculation. The above value of R^{exp} is dominated by two measurements, one made at TRIUMF [5],

$$R_{e/\mu}^{\mathrm{exp}} = [1.2265 \pm 0.0034(\mathrm{stat}) \pm 0.0044(\mathrm{syst})] \times 10^{-4},$$

and the other at PSI [6],

$$R_{e/\mu}^{\mathrm{exp}} = [1.2346 \pm 0.0035(\mathrm{stat}) \pm 0.0036(\mathrm{syst})] \times 10^{-4}.$$

The π_{e2} branching ratio world average presently provides the best test of μ–e universality.

Broader implications of electron–muon $(e$–$\mu)$ universality and of the above value for $R_{e/\mu}^{\mathrm{exp}}$ were discussed in detail in Ref. [7] and are briefly revisited below. Experimental tests of lepton universality provide a useful crosscheck of SM predictions, as well as potentially useful independent limits on masses and couplings of certain particles outside of the SM.

Rapid developments in the neutrino sector in recent years have renewed the interest in lepton universality. Comprehensive reviews of the subject were made by Pich [8] and Loinaz et al. [9]. In all such analyses the e–μ universality limit from the branching ratio of $\pi_{e2(\gamma)}$ decay emerges as the most stringent limit available. This is well illustrated in Fig. 1 which shows a set of four summary plots of the experimental limits on lepton universality from

---

[‡]The "(γ)" appearing in the decay designations implies that the radiative decays $\pi \to \ell\bar{\nu}\gamma$ are not resolved or subtracted from the $\pi \to \ell\bar{\nu}$ yield.

Loinaz et al. [9]. The authors have parametrized possible flavor non-universal suppressions of the SM lepton coupling constants g_ℓ in $W\ell\nu_\ell$ coupling ($\ell = e, \mu, \tau$) as follows:

$$g_\ell \quad \longrightarrow \quad g_\ell \left(1 - \frac{\epsilon_\ell}{2}\right).$$

The linear combinations of ϵ_ℓ's constrained by W, τ, π, K decays are:

$$\frac{g_\mu}{g_e} = 1 + \frac{\epsilon_e - \epsilon_\mu}{2}, \qquad \frac{g_\tau}{g_\mu} = 1 + \frac{\epsilon_\mu - \epsilon_\tau}{2}, \qquad \text{and} \qquad \frac{g_\tau}{g_e} = 1 + \frac{\epsilon_e - \epsilon_\tau}{2}.$$

Two of the three combinations are independent. Experimental constraints can be evaluated on $\Delta_{e\mu} \equiv \epsilon_e - \epsilon_\mu$, $\Delta_{\mu\tau} \equiv \epsilon_\mu - \epsilon_\tau$, and $\Delta_{e\tau} \equiv \epsilon_e - \epsilon_\tau$; Loinaz et al. have chosen the latter two. The corresponding plots are shown in Fig. 1. Improving the π decay limit on g_μ/g_e would have the effect of reducing the allowed region to a narrower strip in the $\Delta_{\mu\tau}$–$\Delta_{e\tau}$ plane.

It is interesting to examine the absolute size of the experimental limits on lepton universality. We start with the ratio of the $\pi_{\ell 2}$ decay rates

$$R_{e/\mu} = \frac{\Gamma(\pi \to e\bar{\nu}(\gamma))}{\Gamma(\pi \to \mu\bar{\nu}(\gamma))} = \frac{g_e^2}{g_\mu^2} \frac{m_e^2}{m_\mu^2} \frac{(1 - m_e^2/m_\pi^2)^2}{(1 - m_\mu^2/m_\pi^2)^2} \left(1 + \delta R_{e/\mu}\right), \tag{1}$$

where $\delta R_{e/\mu}$ denotes the radiative corrections to the processes, amounting to almost four percent. Similarly, the ratio of the relevant τ and π decay rates yields

$$R_{\tau/\pi} = \frac{\Gamma(\tau \to \pi\nu_\tau(\gamma))}{\Gamma(\pi \to \mu\bar{\nu}(\gamma))} = \frac{g_\tau^2}{g_\mu^2} \frac{m_\tau^3}{2m_\mu^2 m_\pi} \frac{(1 - m_\pi^2/m_\tau^2)^2}{(1 - m_\mu^2/m_\pi^2)^2} \left(1 + \delta R_{\tau/\pi}\right), \tag{2}$$

this time with smaller radiative corrections ($\delta R_{\tau/\pi} \simeq 0.0016$). Using the above equations and the available experimental data, one can evaluate [9]

$$\left(\frac{g_e}{g_\mu}\right)_\pi = 1.0021 \pm 0.0016 \quad \text{and} \quad \left(\frac{g_\tau}{g_\mu}\right)_{\pi\tau} = 1.0030 \pm 0.0034.$$

For comparison, W decays yield limits that are almost an order of magnitude less stringent [9]:

$$\left(\frac{g_e}{g_\mu}\right)_W = 0.999 \pm 0.011 \quad \text{and} \quad \left(\frac{g_\tau}{g_e}\right)_W = 1.029 \pm 0.014.$$

It bears noting that a flavor non-universal coupling suppression of the order of a few times 10^{-3} would suffice to account for the NuTeV anomaly [10], provided, of course, that the latter is real [9]. In time, the present NuTeV controversy may come to be resolved otherwise; however, an accurate determination of $R_{e/\mu}$ in pion decay will remain valuable regardless of the future developments in theory and experiment.

In addition to testing lepton universality, precise measurement of the π_{e2} branching ratio can constrain certain other non-standard model scenarios. In particular, if the decay were dominated by a pseudoscalar coupling, then the helicity suppression of the π_{e2} decay would vanish and the branching ratio would be $\Gamma(\pi \to e\bar{\nu}(\gamma))/\Gamma(\pi \to \mu\bar{\nu}(\gamma)) = 5.5$. The difference between the best experimental results and the standard model description of the process
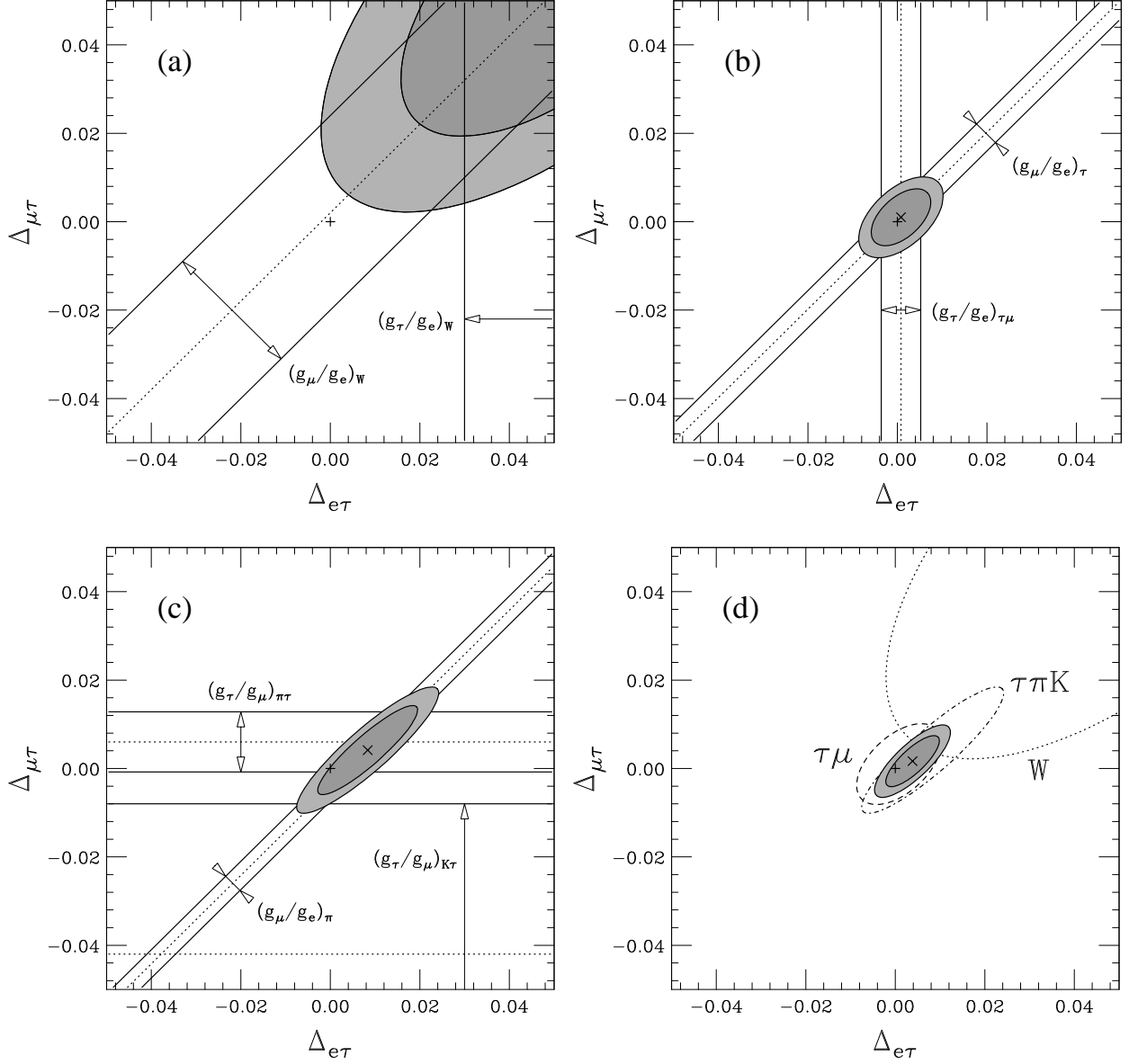
Figure 1: Experimental constraints on possible violations of lepton universality plotted in the $\Delta_{\mu\tau}$ vs. $\Delta_{e\tau}$ (from Loinaz et al., Ref. [9]). Limits in panel (a) are derived from W decay, from τ decay in panel (b), from π and K decay in panel (c). Panel (d) depicts the combined limits. Improving the π decay limits on g_μ/g_e would have the effect of reducing the allowed region to a narrower strip in panels (c) and (d).

provides an estimate of the residual pseudoscalar coupling. A deviation can occur due to: (i) charged Higgs bosons in theories with more Higgs's than in the standard model, with mass m_{h^+}, (ii) pseudoscalar leptoquarks, with mass m_{pl}, (iii) vector leptoquarks, with mass m_{pV}, and (iv) supersymmetric particles entering the loop diagrams. Subtracting the standard model component from the experimental result we obtain the following bounds on C_P, the ratio of pseudoscalar to vector coupling strengths, at the 2σ level:

$$-7 \times 10^{-3} \leq \frac{C_P}{f_\pi m_e} \leq 2.5 \times 10^{-3} \,, \tag{3}$$

where f_π and m_e are the familiar pion decay constant and electron mass, respectively. Using the model-independent technique outlined in Ref. [7], the following limits on the masses for the maximal coupling can be obtained: (i) $m_{h^+} > 2\,\mathrm{TeV}$, (ii) $m_{pl} > 1.3\,\mathrm{TeV}$ and (iii) $m_{pV} > 220\,\mathrm{TeV}$.

Indirect constraints on C_S, the ratio of scalar to vector coupling, discussed in Ref. [11], provide the following results:

$$-1.2 \times 10^{-3} \leq C_S \leq 2.7 \times 10^{-4} \,. \tag{4}$$

Combined with limits on scalar interactions in muon capture, π_{e2} measurements can impose an order of magnitude stronger limit on the scalar coupling than the direct experimental searches.

In conclusion, the large discrepancy between the theoretical and experimental accuracy provides a strong motivation for a new precise measurement of the π_{e2} branching ratio. We outline below a way to reach the uncertainty range of $2 - 5$ parts per 10^4 in several stages. Finally, we note that a measurement of such accuracy would render insignificant the external systematic uncertainty in the pion beta decay branching ratio we reported in Ref. [12].

2.   Experimental method

The measurement discussed in this proposal is a continuation of a program of precise measurements of rare pion and muon decays using the PIBETA detector system. In the first run, 1999–2001 the chief subject of study was the pion beta (π_β) decay, $\pi^+ \to \pi^0 e^+ \nu$, with the goal to achieve $\sim 0.5\,\%$ accuracy in the π_β branching ratio. We used $\pi^+ \to e^+ \nu$ decay events for normalization. The first result of this work, recently published in Ref. [12], has improved the pion beta decay branching fraction accuracy between six- and sevenfold over the previous most accurate measurement. The π_β decay analysis continues, and an improved final result will be forthcoming. We have also reported a fourfold-improved result on the $\pi^+ \to e^+ \nu \gamma$ radiative decay branching ratio, and F_A, the pion axial vector form factor [13]. A dedicated run in 2004, PSI experiment R-04-01, produced further improvements in precision of the pion form factor F_A and F_V, via pion radiative decay [14]. This work measured for the first time ever the momentum dependence of the pion form factors, and it also lay to rest earlier indications of a tensor anomaly [15] – [22]. The 2004 run also resulted in a new measurement of the radiative muon decay branching ratio, and a new upper limit on the Michel parameter $\bar{\eta}$ [24]. This set of measurements has demonstrated that the PIBETA detector system can achieve an absolute sensitivity of a few parts in 10^{11}, which is appropriate to the task at hand.

The experimental method to be used in the proposed π_{e2} measurement builds strongly on that used in the π_β runs. Details of the PIBETA detector architecture and the π_β measurement technique are given in Refs. [12, 13, 23]. In this proposal we reproduce only the most relevant points. Figures 2–4 schematically depict the components and the geometry of the PIBETA detector system.

Of particular interest is Figure 5, which shows the π_{e2} signal definition in the 1999–2001 PIBETA run. The time signature of the $\pi \to e\nu$ events was critical in separating them from the background dominated by muon decays. This method is adequate for counting π_{e2} relative to π_β events with at least 0.3 % accuracy, thanks to much shared systematics. In particular, the undetected low energy "tail" of the π_{e2} calorimeter response was largely correlated with the similar "tail" for the π_β photon showers. The low-energy events in both channels were primarily caused by shower leakage in the back of the CsI calorimeter.

For an absolute measurement of the π_{e2} decay branching ratio we plan to use the following approach:

(i) We will use the lowest feasible pion beam momentum. Tests run in October 2005 indicate that the range $70 - 75\,\mathrm{MeV/c}$ will likely satisfy our requirements.

(ii) We will use the muon decays $\mu \to e\nu\bar{\nu}(\gamma)$ for branching ratio normalization.

(iii) Finally, we will accurately measure the entire energy dependence of the calorimeter response to the decay positrons, the low energy "tail," in a separate, prescaled trigger. The π_{e2} "tail" will be separated from the Michel decay background by applying appropriate cuts on the digitized target pulses.

The π_{e2} events will be collected using a high-threshold one-arm trigger (HT1), already used in the PIBETA experiment. Choice of the threshold energy, discussed below, will be made so as to minimize the fraction of events in the π_{e2} "tail," while keeping the trigger rate acceptable. Using a low beam momentum results in several advantages: (a) reduced thickness of the active degrader detector, with the accompanying reduction in prompt hadronic events, and (b) reduction of the pion stop energy deposition in the target to levels comparable with the $\pi \to \mu\nu$ signal, $\sim 4\,\mathrm{MeV}$. The latter feature enhances the reliability of discrimination of $\pi \to e$ from $\pi \to \mu \to e$ event sequences in the target.

Applying this approach, the π_{e2} branching ratio can be evaluated as

$$B(\pi \to e\nu) \equiv B_{e2} = \frac{N_p(1 + \epsilon)}{A_{e2}\, N_{\pi^+}\, f_{\pi d}(T)} \,, \tag{5}$$

where N_p is the number of recorded π_{e2} events in the peak above the trigger high CsI energy threshold, E_{HT}, $\epsilon = N_t/N_p$ is the ratio of the "tail" to "peak" π_{e2} events, A_{e2} is the detector acceptance, N_{π^+} is the number of stopped beam pions seen by the experiment, while $f_{\pi d}(T)$ is the pion decay probability between the pion stop time, $t = 0$, and the end of the trigger gate, $t = T$, i.e., $f_{\pi d}(T) = 1 - e^{-T/\tau_\pi}$, where τ_π is the pion lifetime. While we can count the stopped pions directly, a more reliable count can be obtained by recording the sequential $\pi \to \mu \to e$ decays:

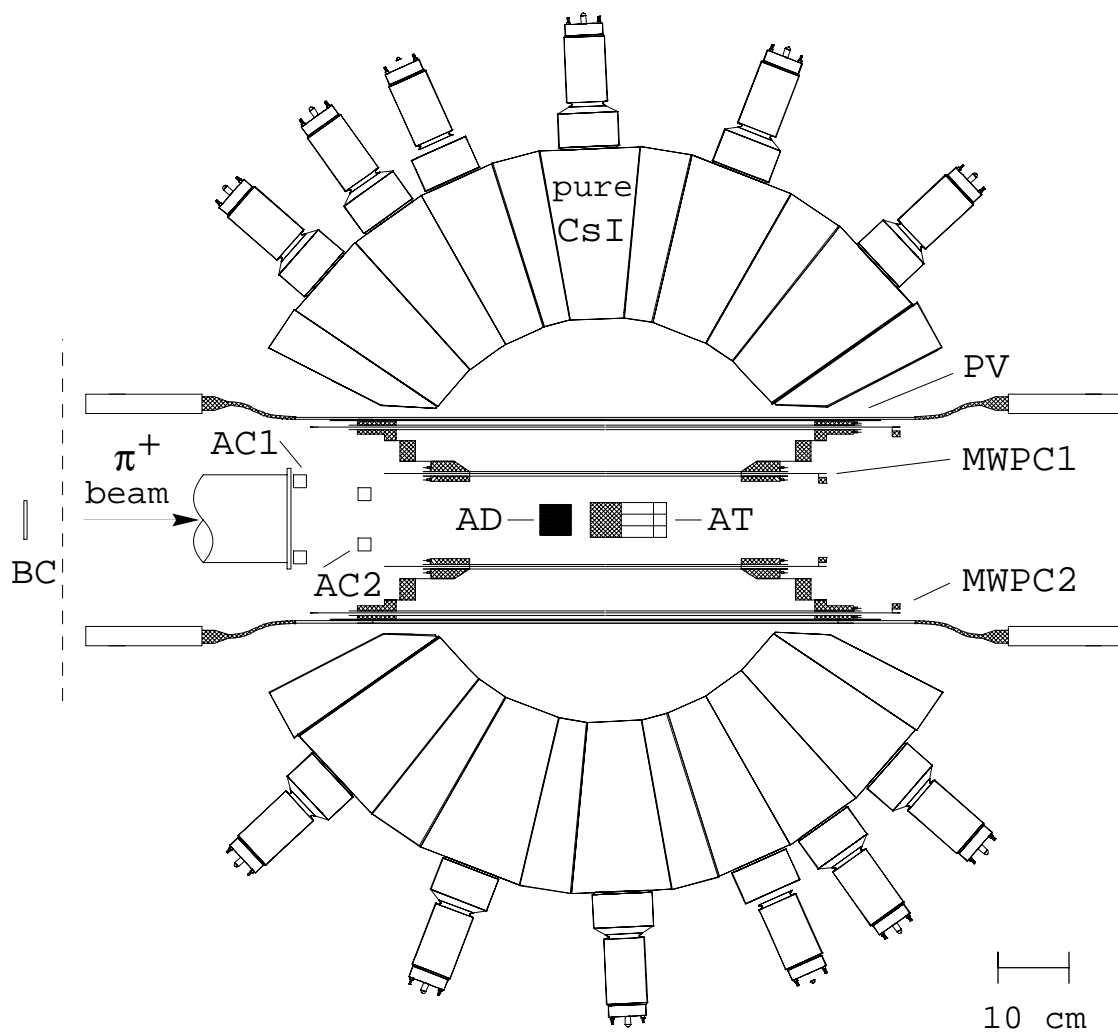$$B_\mu = \frac{N_M}{A_M\, N_{\pi^+}\, f_{sd}(T)} \,, \tag{6}$$

8

Figure 2: (above) Schematic cross section of the PIBETA apparatus showing the main components: beam entry, active degrader and target, MWPC's and support, plastic veto detectors and PMT's, pure CsI calorimeter and PMT's.
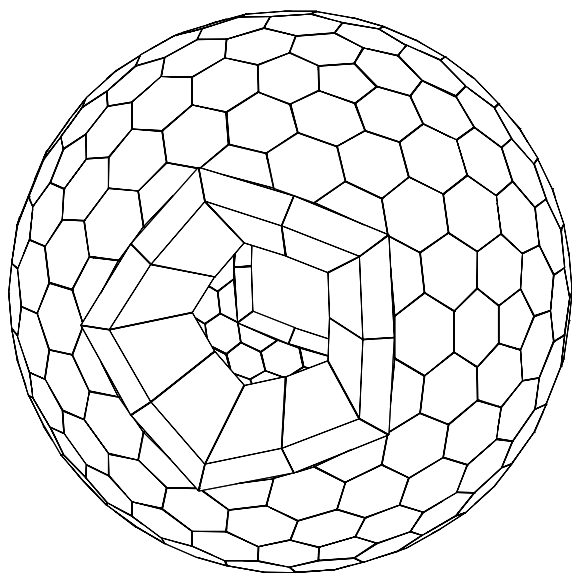
Figure 3: (left) A view showing the geometry of the pure CsI shower calorimeter. The sphere is made up of 240 elements, truncated hexagonal, pentagonal, and trapezoidal pyramids; it covers about $80\,\%$ of 4π in solid angle.
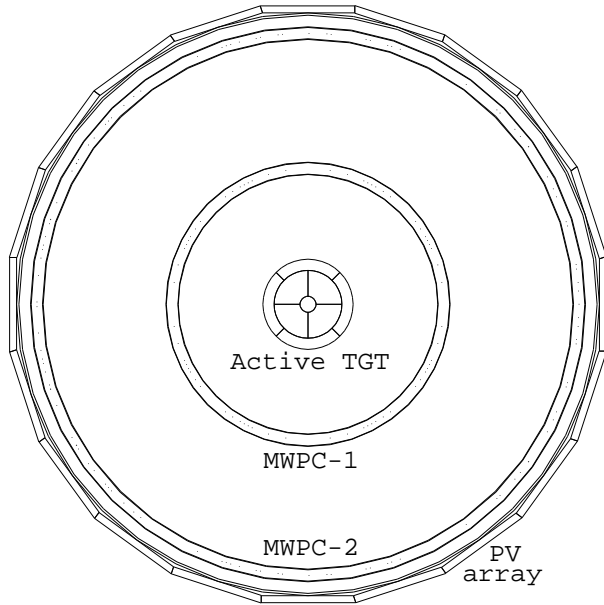
Figure 4: Axial view of the central detector region showing the nine-element target detector, the two thin concentric MWPC's, and the twenty-element thin plastic scintillator barrel veto detector. The nine-element target will be replaced by a single-piece detector for the proposed $\pi \to e\nu$ runs. (Beam is perpendicular to the page.)

where $B_\mu \simeq 1$ is the branching ratio for $\mu \to e\nu\bar{\nu}(\gamma)$ decay, discussed in Sec. 2.2, A_M and N_M are the detector acceptance and number of muon decay events, respectively, and

$$f_{sd}(T) = 1 - \left(\tau_\mu e^{-T/\tau_\mu} - \tau_\pi e^{-T/\tau_\pi}\right)/(\tau_\mu - \tau_\pi) \,, \tag{7}$$

is the probability of sequential decay $\pi \to \mu \to e$ between $t = 0$ and the trigger gate end, $t = T$, where τ_μ is the muon lifetime. Combining the two expressions to eliminate N_{π^+}, we get

$$B_{e2} = \frac{N_p(1 + \epsilon)}{N_M} \cdot \frac{A_M}{A_{e2}} \cdot \frac{f_{sd}(T)}{f_{\pi d}(T)} B_\mu \,, \tag{8}$$

which conveniently factorizes into quantities that share many of the same systematic uncertainties.

2.1. Statistical uncertainties and event rates

Trigger parameters (e.g., length of the trigger gate, choice of E_{HT}, etc.), event rates, and statistical uncertainties are all related, resulting in the need to find an overall optimum. A reasonable goal for the relative statistical accuracy of the branching fraction measurement is 2×10^{-4}. Since $N_M \gg N_p$, counting statistics of Michel events is not a constraint. We therefore focus on the π_{e2} counting statistics.

The total number of π_{e2} events in Eqs. (5) and (8) is determined as: $N_{e2} = (1 + \epsilon)N_p$. Thus, we have for the relative statistical uncertainty

$$\frac{\Delta N_{e2}}{N_{e2}} = \left[\frac{1}{N_p} + \frac{(\Delta\epsilon)^2}{(1 + \epsilon)^2}\right]^{1/2} \,. \tag{9}$$

The tail fraction, ϵ, is measured in a prescaled low-threshold trigger that accumulates the muon decay events, with a prescaling factor f. Thus,

$$\epsilon = \frac{N_t'}{N_p'} \,, \qquad \text{where} \qquad N_t' = fN_t \,, \qquad \text{and} \qquad N_p' = fN_p \,. \tag{10}$$
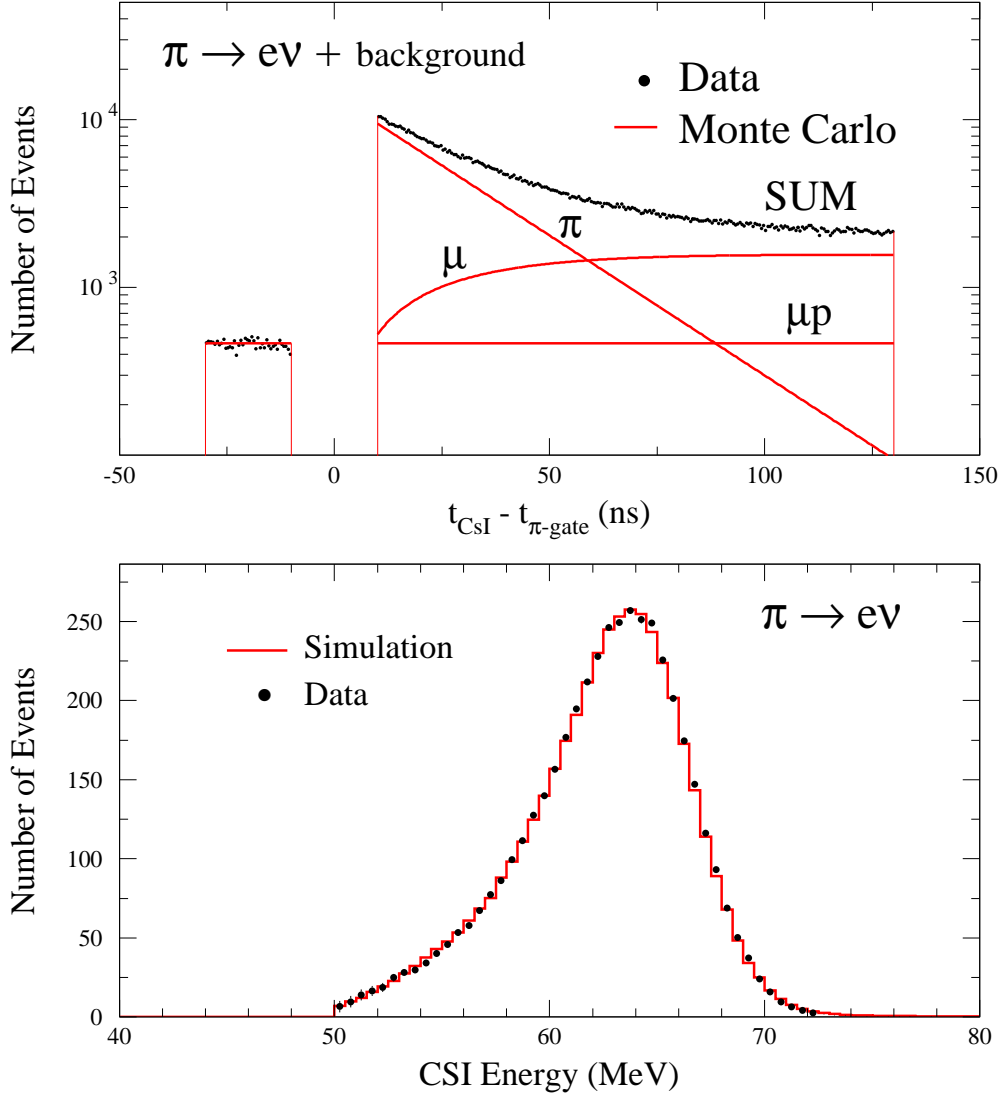
Figure 5: Top panel: A typical histogram (dots) of differences between the positron track time, t_{CsI}, and beam pion stop time, $t_{\pi\text{-gate}}$, for one-arm trigger events, compared with a sum of the Monte Carlo-simulated responses for π_{e2} decay (π), muon decay (μ), and muon pile-up events (μp). The π_{e2} pile-up background, being much lower, is off scale in the plot. Prompt events are suppressed. Bottom panel: CsI calorimeter energy spectrum for the π_{e2} decay events, after background subtraction. The "tail" below 50 MeV was not measured with the same precision as the yield above 50 MeV, and is not shown.
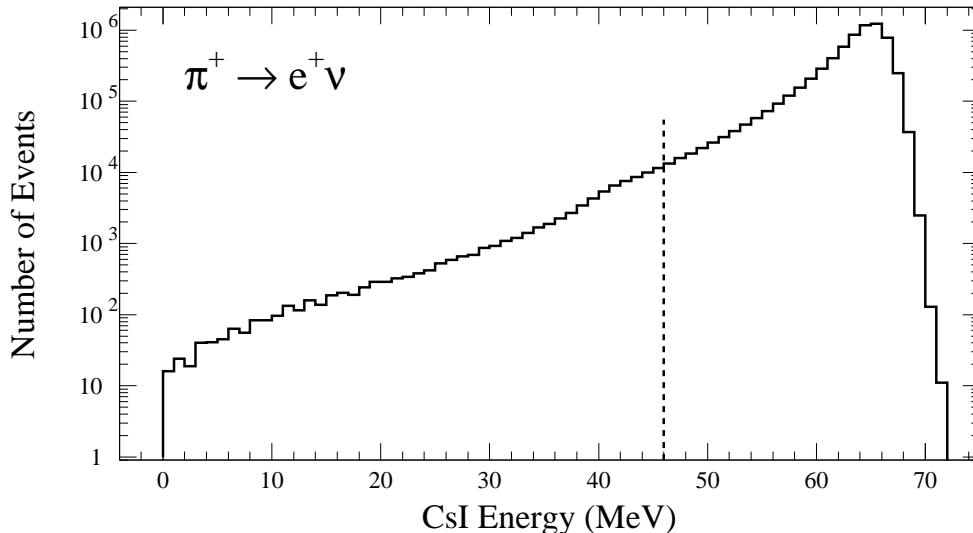
Figure 6: Energy spectrum in the CsI calorimeter for 10^7 $\pi \to e\nu$ decay events simulated in GEANT3 with appropriate cuts on measured observables applied. The vertical dashed line at $46\,\mathrm{MeV}$ denotes the anticipated placement of the HT1 trigger threshold.

The statistical uncertainty of ϵ is, then, given by

$$\Delta\epsilon = \epsilon \left[\frac{1}{N_t'} + \frac{1}{N_p'} \right]^{1/2} . \tag{11}$$

Combining these results, we obtain the relative statistical uncertainty of

$$\frac{\Delta N_{e2}}{N_{e2}} = \left[\frac{1}{N_p} + \frac{\epsilon^2}{N_t'} + \frac{\epsilon^2}{N_p'} \right]^{1/2} = \left[\frac{f + \epsilon + \epsilon^2}{f N_p} \right]^{1/2} . \tag{12}$$

To optimize the above parameters, we need to make further choices regarding the trigger.

Firstly, we will leave the pion gate unchanged from prior running, i.e., the $180\,\mathrm{ns}$ gate will extend from $30\,\mathrm{ns}$ prior to pion stop time ($t = 0$) to $150\,\mathrm{ns}$ after pion stop time.

Secondly, E_{HT}, which was set at approximately $50.5\,\mathrm{MeV}$ in the 2004 run, will be lowered to about $46\,\mathrm{MeV}$, and possibly more. This gives an approximately seven- to eightfold increase of Michel decay events in the one-arm high trigger (HT1). In 2004 the π_{e2} and muon decay events were approximately equal in number in HT1. At 20,000 pion stops/second, the combined muon and π_{e2} decay rate in HT1 would be approximately 5 events/s. Lowering E_{HT} has the important consequence of reducing ϵ, the π_{e2} "tail" fraction to about 0.02. Thus, for the remainder of this document we will use the conservative value of $\epsilon = 0.02$. A realistic simulation of the full $\pi \to e\nu$ energy signal in the CsI calorimeter for 10^7 decays is displayed in Fig 6, along with the $46\,\mathrm{MeV}$ threshold.

Using Eq. (12), $\Delta N_{e2}/N_{e2} = 2 \times 10^{-4}$, and $r_{\pi\mathrm{stop}} = 20{,}000\,\mathrm{s}^{-1}$, we readily obtain the values of running parameters listed in Table 1. (The overall trigger rate is dominated by the prescaled low-threshold one-arm, LT1, trigger event rate.)

Table 1: Values of N_p, number of π_{e2} events in HT1 trigger, f, prescaling factor for LT1 trigger, r_{trig}, overall trigger rate, all with $\epsilon = 0.02$, $\Delta N_{e2}/N_{e2} = 2 \times 10^{-4}$, 20,000 π_{stop}/s, and pion gate ending at $T = 150\,\text{ns}$ after pion stop time.

N_p	f	$r_{\text{trig}}\ (\text{s}^{-1})$
2.7×10^7	1/4	~ 280
2.9×10^7	1/8	~ 145
3.4×10^7	1/16	~ 75
4.4×10^7	1/32	~ 45

Table 1 clearly demonstrates that the PIBETA detector system, used in the mode as described, is capable of reaching statistical uncertainty levels in π_{e2} decay that are an order of magnitude better than those obtained in previous experiments, all with reasonable beam and event rates. At $R_{\pi\text{stop}} = 2 \times 10^4$/s, it would take about 1.5×10^7 s, or six months, of net beam time to record $N_p = 3 \times 10^7$ π_{e2} events. Certain improvements in our data acquisition system will be required in order to realize the running conditions outlined above. These improvements can be implemented using existing technology.

We close the section on counting statistics and trigger rates with a comment regarding the strong-interaction prompt background. In our 2004 runs, with beam momentum of $\sim 115\,\text{MeV}/c$, we registered one prompt event for approximately 5,000 pion stops. At the reduced beam momentum of $\sim 75\,\text{MeV}/c$, the prompt rate will be reduced by more than an order of magnitude. Because of its negative reaction Q-value, pion single charge exchange on carbon nuclei in the target will be virtually eliminated at the lower beam momentum, and pion absorption induced events, originally $\sim 15\,\%$ of the prompt data sample at $115\,\text{MeV}/c$, will be reduced by at least a factor of four. Thus, we expect prompt reactions to contribute about one event per second, or fewer, to the trigger rate.

2.2. Systematic uncertainties

Having demonstrated that meaningful statistical uncertainties can be reached using our technique, we turn to the systematic uncertainties, which typically place more stringent demands on the experiment. We take Eq. 8 as the starting point, and discuss each term separately.

Pion and muon decay event discrimination

At 20,000 pion stops/second and below, muon pileup in the target is negligible. Successive pions are separated on average by $50\,\mu$s, or almost 23 muon lifetimes, resulting in muon pileup probability of just over 10^{-10}. However, as seen in Figure 5, muon pileup has a distinct time signature and would be reliably accounted for even if it were not negligible.

Key to accomplishing reliable pion/muon decay discrimination is to make use of digitized target, degrader and forward beam counter waveforms. In terms of simple energy resolution, already $\sigma_E \simeq 700\,\text{keV}$ in the target detector signal integrated charge (or just ~ 40 photo-

electrons/MeV) would result in failure to identify the intermediate muon pulse in sequential $\pi \to \mu \to e$ decay with $< 2 \times 10^{-4}$ probability. We believe we can do better, even after folding in effects of noise, which will be independently minimized. In addition, we will have at our disposal waveform fits which sharpen the sensitivity compared to testing the integrated charge alone. Finally, misidentified events erroneously assigned to the wrong data set (π_{e2} or $\pi \to \mu \to e$) would have the wrong overall time and energy distributions. Of the two failure modes, the former is potentially more significant. The $t \simeq T$ region in the π_{e2} sample provides the necessary sensitivity to misidentified events at the level below 10^{-4}. The task of pion and muon decay separation is made much easier by using lower beam momenta which reduce the pion stop signal in the target to a size comparable with the $4\,\mathrm{MeV}$ muon energy loss signal in $\pi \to \mu$ decay.

Uncertainties in the muon decay normalization

Excluding effects of radiative decays which are discussed below, there are several sources of uncertainty associated with the normalization to muon decay and the necessity of a nonzero energy threshold for the LT1 trigger. Thanks to recent work by the TWIST collaboration, the Michel parameter ρ is now known with 10^{-3} precision [25]

$$\rho = 0.7508 \pm 0.0010\,. \tag{13}$$

Translated to an integral uncertainty above a given threshold, this result requires that the threshold be below $20\,\mathrm{MeV}$ in order for $\Delta N_M/N_M \leq 1 \times 10^{-4}$. Even our previous PIBETA runs with a threshold of about $5\,\mathrm{MeV}$ would satisfy this constraint.

A more stringent requirement stems from the limited accuracy of our energy calibration. In prior PIBETA running we achieved the energy scale uncertainty of 2×10^{-3} for charged particles (positrons). Conservatively assuming no improvement in this number, a $5\,\mathrm{MeV}$ threshold would result in $\Delta N_M/N_M = 1 \times 10^{-4}$. Planned changes in our data acquisition electronics (elimination of CsI signal splits for the now defunct waveform digitizer) will enable us to implement a $1\,\mathrm{MeV}$ threshold, that will satisfy the above constraint conservatively.

Ratio of acceptances for π_{e2} and Michel decay events

This is the term where most systematics, such as particle identification inefficiencies, tracking resolution and efficiency, etc., are strictly shared. In addition, our prior work has demonstrated that we have excellent control of the instrumental efficiencies, anyway. Potentially significant differences arise from two sources mainly: (non)inclusion of radiative events, and nuclear interactions of particles in electromagnetic showers in CsI. We discuss each below.

Role of radiative decays, B_μ

Normally, weak decay branching ratios, both calculated and measured, of necessity include contributions of radiative processes (inner bremsstrahlung), since, strictly speaking, there is no such thing as nonradiative decay. The PIBETA calorimeter can differentiate radiative events with photons above a certain energy threshold, and with angle to the positron greater

than a certain cutoff value. In past analyses these were chosen to be 10 MeV and 30°, respectively. The PIBETA experiment has, in fact, produced the most accurate measurements of the $\pi \to e\nu\gamma$ and $\mu \to e\nu\bar{\nu}\gamma$ branching ratios with uncertainties of 10^{-4} or better relative to the main "nonradiative" decay branching ratios [13, 14, 24]. A case in point is our result for radiative muon decay with $E_\gamma \geq 10$ MeV and $\theta_{e\gamma} \geq 30°$ [24]:

$$B(\mu \to e\nu\bar{\nu}\gamma) = [4.40 \pm 0.02(\text{stat}) \pm 0.09(\text{syst})] \times 10^{-3}, \tag{14}$$

where the systematic error is set conservatively high to account for the uncertain GEANT3 description of low-energy large-angle bremsstrahlung processes, as they impact the acceptance. We have plans to improve our simulation of bremsstrahlung, which will bring the above systematic uncertainty in line with the statistical one. Radiative decays with smaller positron-gamma opening angles and softer photons are included in the nominal $\mu \to e\nu\bar{\nu}(\gamma)$ decay sample. Hence, at present our prior work provides an effective measurement of B_μ with sub-10^{-4} accuracy. The PEN experiment, with its planned large sample of muon decays, will offer an opportunity to improve our muon radiative decay result further.

Role of nuclear interactions in the detector

Nuclear interactions in CsI induced by electromagnetic shower particles will impact the two decays differently because of the difference in the shower energies in muon and pion decay. The effect of nuclear interactions will be a very slight softening of the recorded shower energy spectra due to energy losses to processes with lower detection efficiency, like neutron emission. The effect is more pronounced in pion decay. Calculations with FLUKA and GEISHA programs for π_{e2} showers indicate that the overall probability for these processes is below about 0.8 %, while the effect on the π_{e2} "tail" is lower by an order of magnitude. Hence, we need to understand and quantify this effect at about 10 % level, which we believe to be feasible. We plan a program of improving the accuracy of our simulation of photo- and electronuclear processes in a systematic way. Partly for this reason, as well as for others, we plan to switch our detector simulation to GEANT4 which offers certain advantages over GEANT3.

Time-zero definition and ratio $f_{\pi d}(T)/f_{sd}(T)$

This systematic has two aspects: precise definition of pion stop time, $t = 0$, and absolute calibration of the time scale, i.e., the actual value of $t = T$, the gate cutoff, in nanoseconds.

Unlike our higher-rate PIBETA running, in the PEN experiment we will not apply a PROMPT veto in the main triggers (HT1, LT1, etc.). In practice, that means that the gap around $t = 0$ visible in the top panel of Figure 5 will not be present in the PEN data set, giving us a direct measurement of $t = 0$. Furthermore, the most accurate timing will be extracted from the digitized target pulses. However, we have to consider the possibility of a systematic offset between the $t = 0$ points in the π_{e2} and $\pi \to \mu \to e$ data samples. Keeping the associated relative error under 2×10^{-4} imposes the requirement that the relative offset be known with a precision of 5 ps. While this is by no means a trivial goal, we expect that we will be able to approach, and eventually realize it. For comparison, in our 2004

data set we achieved $22\,\mathrm{ps}$ resolution of the $t = 0$ point using standard scintillator material, standard fast photomultiplier tubes, and TDC timing. In the PEN experiment we intend to use specialized fast scintillator for the target, microchannel plate light readout, and a multi-GHz waveform digitizer with short signal cable runs for maximum signal bandwidth preservation. In addition, we are developing systematic checks to sharpen our sensitivity to the $t = 0$ offset problem.

The timescale calibration, i.e., measurement of T, is an easier task thanks to periodic accidental pion stops in the target. The accelerator radio-frequency (rf) pulse structure provides a very precise timebase. The $180\,\mathrm{ns}$ pion gate will accommodate at least seven fully resolved pion stop peaks with $19.750042(4)\,\mathrm{ns}$ spacing. The probability for a pion to reach the target in time with any one of these beam pulses is 4×10^{-4}. In the planned sample of $\sim 10^9$ triggers, we should acquire about a half-million counts in each periodic beam pulse. In previous PIBETA runs, using standard equipment and methods, we were able to reach picosecond precision level, sufficient for the present needs. With improved equipment and technique in the PEN experiment we will do even better.

Summary of systematic errors

We have identified and discussed the main sources of systematic uncertainties. These systematic effects are uncorrelated. Some of them we already control, while for others we have a clear program of simulation and measurement improvements, that would bring each contribution down to the level of 10^{-4} or lower. We conclude that an overall systematic uncertainty in the neighborhood of $2 - 3 \times 10^{-4}$ represents an attainable, if very challenging, goal.

2.3. Beam and detector improvements

Several modifications are required to bring the PIBETA apparatus to a state that would meet the PEN experiment requirements.

Low momentum beam tunes

Pion beam tunes with momentum in the range $65 - 80\,\mathrm{MeV/c}$ were developed and successfully tested in the October 2005 πE1 area beam development run. Sample time-of-flight spectra between an upstream beam counter (BC, $2\,\mathrm{mm}$ thick plastic scintillator) and the active degrader counter (AD, $5\,\mathrm{mm}$ thick plastic scintillator), separated by about $3.5\,\mathrm{m}$ flight path, for five beam momenta are shown in Fig. 7. This figure clearly illustrates the $e/\mu/\pi$ TOF separation and relative abundance as a function of momentum. The measured pion stop intensities meet the requirements of the π_{e2} measurement.

Further evidence of excellent $e/\mu/\pi$ separation is given in Fig. 8. Positrons, muons and pions are well resolved for all TOF values. These data were acquired in the latter part of the October 2005 beam time, in which we used a NaI calorimeter to help distinguish pion decays. The NaI detector acceptance was defined by a $10\,\mathrm{cm} \times 10\,\mathrm{cm} \times 1\,\mathrm{cm}$ plastic scintillation counter placed at $36\,\mathrm{cm}$ distance from the center of the target counter, its axis at $\theta \simeq 47°$ to the beam.
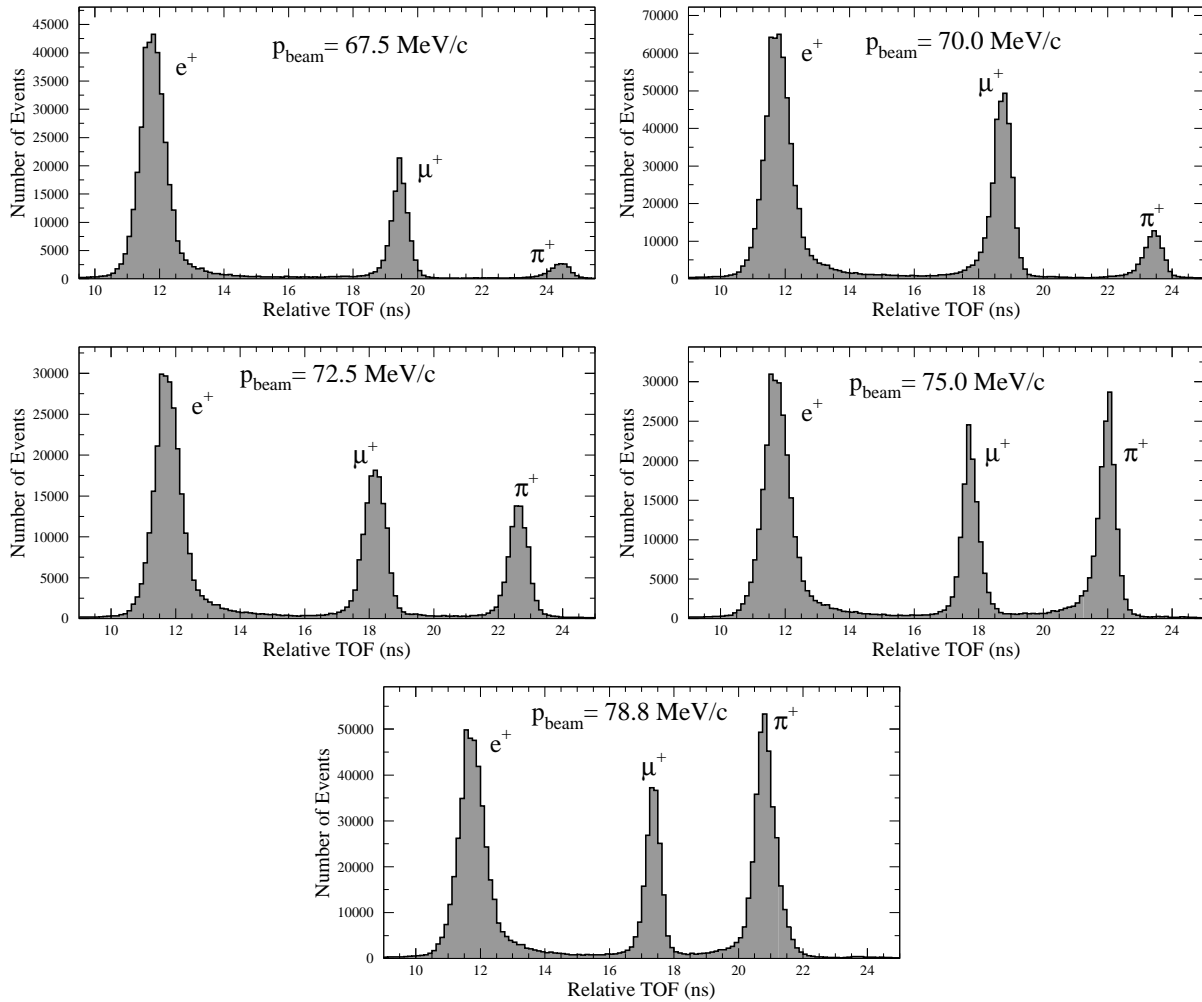
Figure 7: Relative time-of-flight (TOF) for e^+, μ^+, and π^+ particles between the forward beam counter BC (5 mm thick plastic scintillator) and target (15 mm thick plastic scintillator) for five beam momenta. Data collected in the October 2005 beam development run.
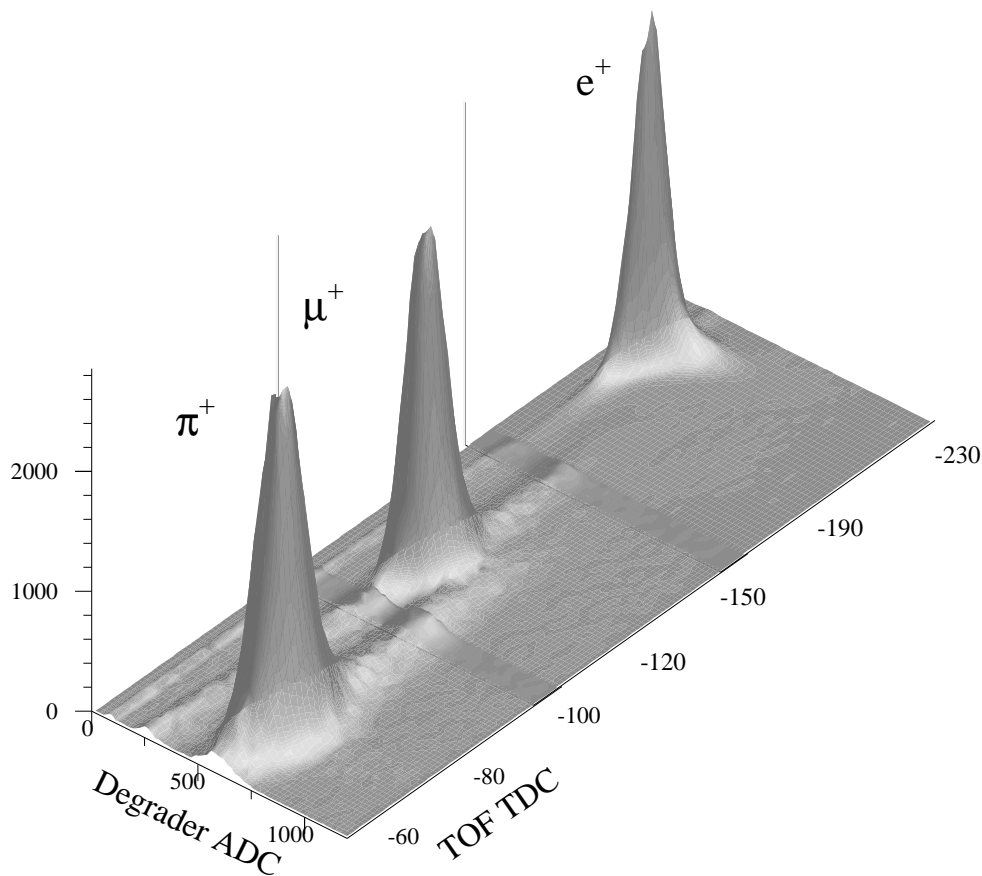
Figure 8: Relative time-of-flight (TOF) for e^+, μ^+, π^+ between the forward beam counter BC and degrader detector, displayed against prompt energy deposited in the degrader counter. Events are selected by requiring a hit in the NaI calorimeter. We note the excellent separation of the three particle species at all times of flight. Data collected in the October 2005 beam development run.
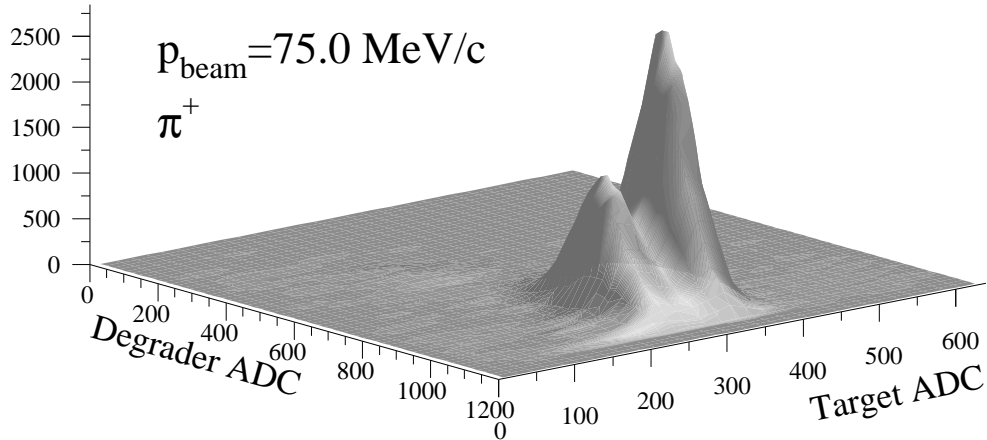
Figure 9: Two-dimensional plot of prompt energy deposited in the degrader and target counters clearly distinguishes events with early $\pi \to \mu$ decay during the $\sim 30\,\mathrm{ns}$ long ADC gate (large peak) from those accompanied by a later decay. The two peaks differ in deposited energy by about $4\,\mathrm{MeV}$, the kinetic energy of the muon in $\pi_{\mu2}$ decay. Data were collected in the October 2005 beam development run.

Fig. 9 indicates the separation of early $\pi_{\mu2}$ decay events at $75\,\mathrm{MeV/c}$, a critical requirement discussed in the section on systematics. With proper care in the final target detector design, and by using a fast waveform digitizer, we expect no problems meeting the requirement on $\pi_{\mu2}$ decay event identification.

Finally, we note the good separation of $\pi_{\mu2}$ and π_{e2} events in the beam development run, shown in Fig. 10, where the NaI calorimeter was used to measure positron energy in conjunction with the active target counter.

The low momentum beam tunes will be refined with the PIBETA detector assembled and in place in the πE1 area.

Detector and data acquisition upgrades

Several new detector components, as well as electronics upgrades are planned, some of which have already been prototyped and tested. We list them below.

- New thin active target (AT) and degrader (AD) detectors, as well as the upstream beam counter (BC) have been prototyped. All will use fast scintillator materials, the target will be read out by microchannel plates. A new beam counter was successfully used in the October 2005 beam development time. Target and degrader detectors remain under development.

- A new multi-GHz waveform digitizer will be implemented for the AT, AD and BC detectors. The waveform digitizer will be mounted very close to the detector to minimize signal cable length and preserve bandwidth. The existing domino sampling chip (DSC) system is not adequate to the task and must be replaced.
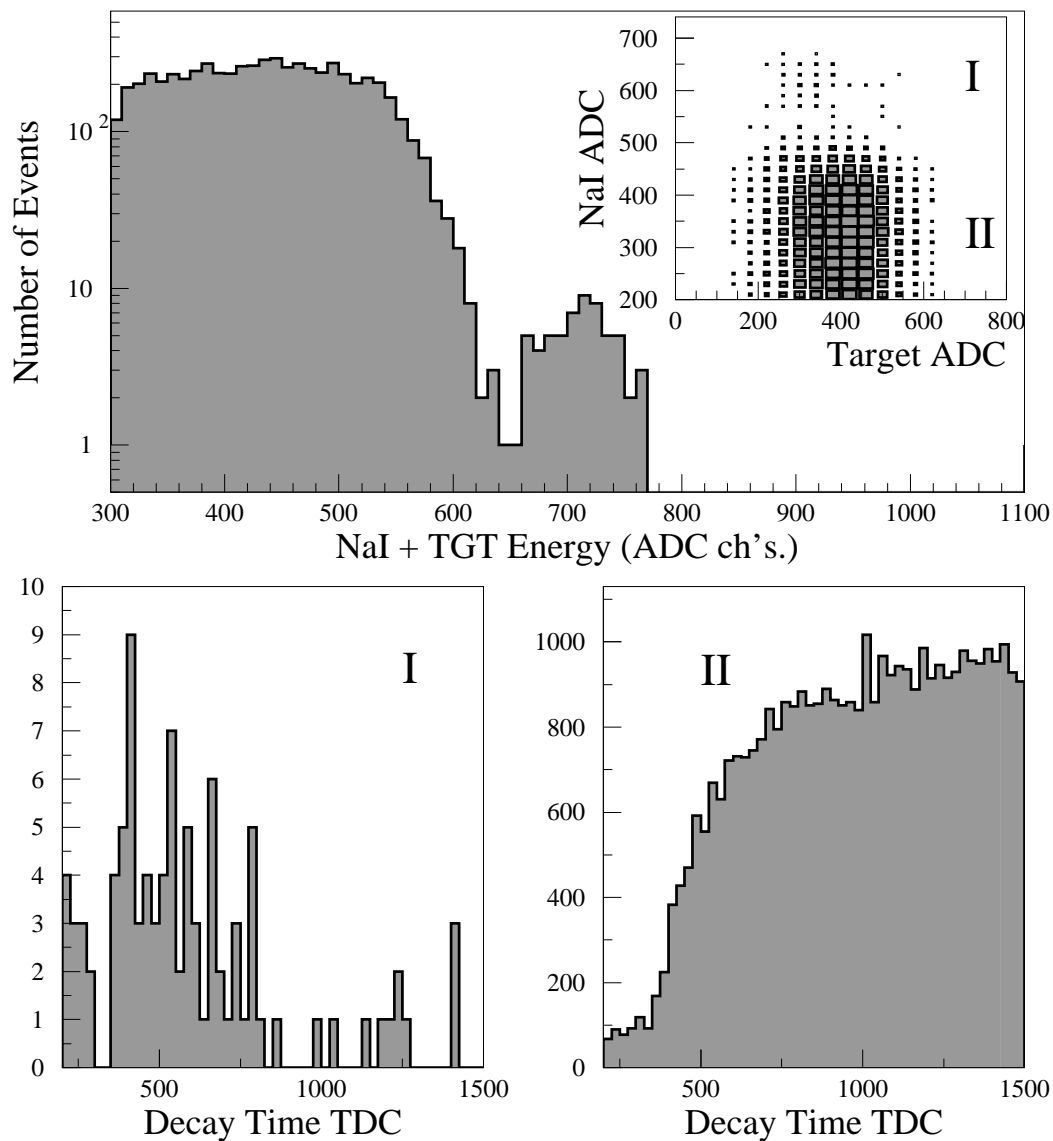
Figure 10: Sum of energies deposited in the NaI and target detectors for delayed decay events recorded over several hours during the October 2005 beam development run (top panel). We note the good separation of π_{e2} and Michel decay events. Region I, dominated by π_{e2} decays, shows an exponential decay time spectrum (lower left panel). Region II, dominated by muon decays, displays the characteristic sequential decay time dependence (lower right panel).

- A new high voltage supply and control system is needed to replace the failing LeCroy 1400 series system now in place. Besides being unreliable, the LeCroy system does not have level of control and stability required in the PEN experiment.

- The trigger electronics will need to be modified and streamlined. It will need to integrate the new waveform digitizer, as well as ensure low deadtime with the planned pion stopping rates.

- Four failing detectors in the CsI calorimeter were repaired in June 2005. The mounting hardware problems which led to slight misalignment of the four photomultiplier tubes were corrected.

3. Project schedule, resources and beam request

The PEN experiment will be conducted in several runs. This will allow us to implement the hardware modifications in a managed way, as well as to assess and control the systematics at increasing levels of accuracy.

We therefore request six weeks of beam time in the πE1 beam area in the fall of 2006, with the option of using it in two separate periods, subject to reconciling potential scheduling conflicts.

There are no major costs to PSI associated with the PEN program. An exception is the new high voltage system. The PSI-developed and built HV system offers adequate stability, and is much more economical than the commercially available alternatives. Its projected cost is 30 kCHF.

We currently plan to fund other non-negligible equipment upgrade costs from sources outside of PSI.

Recurring expenditures include minor material costs and incidental expenses, such as gas for wire chambers, estimated at about 20 kCHF per year, or less.

The current collaboration consists of the collaborators who were active participants in the 2004 run of experiment R-04-01. We are open to new collaborators from outside institutions, as well as PSI. Due to funding realities, it may be necessary to provide modest support for the Swierk and Zagreb collaborators while at PSI. Thanks to improved funding at JINR, the Dubna collaborators would not require similar support.

References

1. W. J. Marciano and A. Sirlin, Phys. Rev. Lett., **71**, 3629 (1993).

2. R. Decker and M. Finkemeier, Nucl. Phys. B **438**, 17 (1995).

3. E.A. Kuraev, JETP Lett. **65**, 127 (1997) [hep-ph/9611294].

4. S. Eidelman et al. (the Particle Data Group), Phys. Lett. B **592**, 1 (2004).

5. D.I. Britton, S. Ahmad, D.A. Bryman, R.A. Burnham, E.T.H. Clifford, P. Kitching, Y. Kuno, J.A. MacDonald, T. Numao, A. Olin, J-M. Poutissou, and M.S. Dixit, Phys. Rev. Lett. **68**, 3000 (1992).

6. G. Czapek, A. Federspiel, A. Flückiger, D. Frei, B. Hahn, C. Hug, E. Hugentobler, W. Krebs, U. Moser, D. Muster, E. Ramseyer, H. Scheidiger, P. Schlatter, G. Stucki, R. Abela, D. Renker, and E. Steiner, Phys. Rev. Lett. **70**, 17 (1993).

7. D.A. Bryman, Comments Nucl. Part. Phys. **21**, 101 (1993).

8. A. Pich, e-Print archive hep-ph/0206011; also Nucl. Phys. Proc. Suppl. **123**, 1 (2003) [hep-ph/0210445].

9. W. Loinaz, N. Okamura, S. Rayyan, T. Takeuchi, and L.C.R. Wijewardhana, Phys. Rev. D **70**, 113004 (2004) [hep-ph/0403306].

10. [NuTeV collaboration] G.P. Zeller et al., Phys. Rev. Lett. **88**, 091802 (2002); Phys. Rev. D **65**, 111103 (2002); e-Print archive hep-ex/0205080.

11. B.A. Campbell, D. W. Maybury, Nucl. Phys. B **709**, 419 (2005).

12. [PIBETA collaboration] D. Počanić et al., Phys. Rev. Lett. **93**, 181803 (2004).

13. [PIBETA collaboration] E. Frlež et al., Phys. Rev. Lett. **93**, 181804 (2004).

14. M. A. Bychkov, Ph.D. thesis, University of Virginia, online at *http://pibeta.phys.virginia.edu/docs/publications/max_thesis/thesis.pdf*, (2005).

15. V. N. Bolotov, S. N. Gninenko, R. M. Dzhilkibaev, V. V. Isakov, Yu. M. Klubakov, V. D. Laptev, V. M. Lobashev, V. N. Marin, A. A. Poblaguev, V. E. Postoev, and A. N. Toropin, Phys. Lett. B **243**, 308 (1990).

16. V. N. Bolotov S. N. Gninenko, R. M. Dzhilkibaev, V. V. Isakov, Yu. M. Klubakov, V. D. Laptev, V. M. Lobashev, V. N. Marin, A. A. Poblaguev, V. E. Postoev, and A. N. Toropin, Yad. Fiz. **51**, 717 (1990) [Sov. J. Nucl. Phys. **51**, 455 (1990)].

17. A. A. Poblaguev, Phys. Lett. B **238**, 108 (1990).

18. A. A. Poblaguev, Phys. Lett. B **286**, 169 (1992).

19. P. Herczeg, Phys. Rev. D **49**, 247 (1994).

20. M. V. Chizhov, Mod. Phys. Lett. **A8** (1993) 2753; hep-ph/0307100; hep-ph/0310203.

21. M. V. Chizhov, hep-ph/0311360.

22. A. A. Poblaguev, Phys. Rev. D, **68**, 054020 (2003).

23. [PIBETA collaboration] E. Frlež et al., Nucl. Instrum. Meth. in Physics Research A **526**, 300 (2004).

24. B. A. VanDevender, Ph.D. thesis, University of Virginia, online at *http://pibeta.phys.virginia.edu/docs/publications/brent_diss.pdf*, (2005).

25. J.R. Musser et al., Phys. Rev. Lett. **94**, 101805 (2005).

26. PIBETA home page: http://pibeta.phys.virginia.edu.